Mon. Not. R. astr. Soc. (1982) **200**, 293–312

Detailed observations of NGC 4151 with *IUE* – II. Variability of the continuum from 1978 February to 1980 May, including X-ray and optical observations★

G. C. Perola[1], A. Boksenberg[2], G. E. Bromage[3], J. Clavel[4], M. Elvis[5], A. Elvius[6], P. M. Gondhalekar[3], J. Lind[7], C. Lloyd[8], M. V. Penston[8], M. Pettini[8], M. A. J. Snijders[2], E. G. Tanzi[9], M. Tarenghi[10], M. H. Ulrich[10] and R. S. Warwick[11]

[1] *Istituto Astronomico dell'Università, Rome, Italy*
[2] *Department of Physics and Astronomy, University College London*
[3] *Astrophysics Group, Rutherford and Appleton Laboratories, Didcot, Oxfordshire*
[4] *Observatoire de Meudon, Meudon, France*
[5] *Harvard-Smithsonian Centre for Astrophysics, Cambridge, Mass., USA*
[6] *Stockholm Observatory, Saltsjöbaden, Sweden*
[7] *Lund Observatory, Lund, Sweden*
[8] *Royal Greenwich Observatory, Hailsham, Sussex*
[9] *Istituto di Fisica Cosmica, CNR, Milano, Italy*
[10] *European Southern Observatory, Garching bei München, Germany*
[11] *Department of Physics, X-ray Astronomy Group, Leicester*

Received 1981 November 26; in original form 1981 July 27

Summary. NGC 4151 has been extensively monitored with *IUE* from 1978 February to 1980 May. The rather erratic behaviour of the ultraviolet light curve seems to be mainly due to variations which occur at rates which, if extrapolated, would produce factor two changes in time-scales between five and 30 days, implying a radius of the order of 0.01 pc for the source. The shape of the continuum can be described by a power law longward of $\lambda 2200$ and by an excess above the extrapolation of that law at shorter wavelengths, suggesting the presence of two components. The long wavelength spectrum becomes harder when the flux increases. The relationship of the short wave excess to the long wavelength component depends on the reddening assumed in the fitting and extrapolation of the power law. According to the assumptions made, the excess is either constant or anticorrelated with the long wavelength flux but a small number of 'anomalous' states exist when the short wavelength excess is absent or weaker than otherwise expected.

★ Ultraviolet data based on observations with the *International Ultraviolet Explorer* collected predominantly at the European Space Agency's Villafranca Satellite Tracking Station.

Measurements made with the Fine Error Sensor on *IUE* and photographically at the RGO show that the variations in the optical flux are fairly closely correlated with those in the mid-ultraviolet (λ2500).

X-ray observations (2-10 keV) made with the SSI on *Ariel V* and with the MPC on the *Einstein Observatory* are compared with those in the ultraviolet. The standard deviation about the mean flux is similar in the two bands (about 30 per cent) but the shortest time-scale in the X-ray variations for large outbursts probably is one order of magnitude shorter than in the ultraviolet. Furthermore, during a large ultraviolet outburst (1979 May) simultaneous X-rays observations showed no sign of strong activity. The implications are that the X-rays come from a much smaller region than the ultraviolet photons and that either energetic events occurring in the two bands are not correlated, or that the manifestations of the same event in the two bands are separated either a few or alternatively more than 10–15 days.

Some implications for current theoretical models are discussed and suggestions for further observational work are given.

1 Introduction

Based on low dispersion data acquired during the first year of operation of the *International Ultraviolet Explorer* (*IUE*) satellite, Penston *et al.* (1981, hereinafter Paper I) described the complex nature of the ultraviolet spectrum of the nucleus of NGC 4151, and identified the main properties of the various spectral components (continuum, emission and absorption lines), with particular regard to their time variability. Those data consisted of observations made at intervals of the order of a month, and it was recognized that, in order to explore the detailed temporal behaviour of the spectral components and the possible existence of correlations between them, further monitoring was needed, at intervals between an hour and a month. This programme, carried out between 1979 May and 1980 May, is unique in providing very extensive data from detailed monitoring of the ultraviolet spectrum ($1150 < \lambda < 3200$ Å) of an active galactic nucleus, and has revealed that significant and often large variations occur in NGC 4151 over intervals of one to a few days.

Our results will be presented and discussed separately for the continuum, the emission lines and the absorption lines. This paper concerns the continuum, and also contains simultaneous or nearly simultaneous measurements made in the optical with the *IUE* Fine Error Sensor (FES) and the 26-inch Thompson refractor at the Royal Greenwich Observatory, and in 2–10 keV X-rays with the *Ariel V* Sky Survey Instrument (SSI) and the *Einstein Observatory* Monitor Proportional Counter (MPC). This has made it possible, for the first time, to search for correlations in the temporal behaviour in the three frequency bands.

2 *IUE* data description

The *IUE*, an ultraviolet spectroscopy satellite, is described by Boggess *et al.* (1978a, b). The low dispersion images used in this paper are listed in Table 1, which includes those already described in Paper I, and others (indicated by (+)) which were retrieved from the *IUE* data bank. Table 1 contains the starting time and duration of each exposure, the aperture used (L = large, S = small), and, when available, the optical magnitude (at about λ4800) m_{FES}, measured during the observing shift with the *IUE* Fine Error Sensor.

All the images were processed and reduced in a uniform way: for the LWP images we

Table 1. Journal of observations. ((x): Pseudo-trailed spectra using three exposures at different positions in the large aperture.)

Date	Image	Ap	Exp time (min)	m_{FES}
1978				
Feb 11.82	SWR 1025	L	60	
12.	LWP 1028	L	120	
28.70	SWR 1064	L	120	
Apr 16.85	LWR 1324 (+)	L	50	
16.90	SWP 1371 (+)	L	40	
16.94	LWR 1325 (+)	L	60	
16.99	SWP 1372 (+)	L	40	
17.02	LWR 1326 (+)	L	40	
17.00	SWP 1373 (+)	S	20	
May 08.29	SWP 1505	S	40	
09.28	LWR 1463	S	60	
11.05	SWP 1518	S	240	11.97 ± .03
11.28	SWP 1519	S	60	
12.05	SWP 1523	S	120	
12.14	LWR 1476	S	120	
12.23	SWP 1524	S	120	
Jun 17.51	SWP 1800 (+)	S	80	
17.58	SWP 1801 (+)	S	30	
Jul 24.85	LWR 1885	L	30	12.13 ± .03
24.89	SWP 2098	S	60	
24.93	SWP 2098	L	30	
Aug 02.09	SWP 2171	L	30	12.01 ± .03
Oct 19.68	SWP 3048	S	60	12.04 ± .03
19.73	SWP 3048	L	30	
19.75	LWR 2650	L	25	
19.77	SWP 3049	L	25	
19.80	LWR 2651	L	25	
31.95	LWR 2782 (+)	S	80	
31.99	SWP 3198 (+)	S	50	
Dec 09.47	LWR 3129	L	30	12.05 ± .03
09.49	SWP 3557	L	30	
09.52	SWP 3557	S	60	
09.56	LWR 3130	L	60	
1979				
Jan 21.53	LWR 3538	L	25	12.23 ± .03
21.55	SWP 3971	L	25	
21.57	SWP 3971	S	60	
21.62	LWR 3539	L	25	
21.64	SWP 3972	L	25	

Date	Image	Ap	Exp time (min)	m_{FES}
1979				
May 03.22	SWP 5100	L	25	
03.24	LWR 4450	L	25	
03.27	SWP 5101	L	25	12.15 ± .03
03.29	LWR 4451	L	25	
03.31	SWP 5102	L	25	
04.64	SWP 5118 (+)	L	20	
19.03	SWP 5296	L	32	
19.06	LWR 4543	L	25	
19.08	SWP 5297	L	50	
19.12	LWR 4544	L	37	
19.14	SWP 5298	L	32	
19.17	LWR 4545	L	22	12.12 ± .03
19.19	SWP 5299	L	50	
19.23	LWR 4546	L	37	
19.26	SWP 5300	L	25	
19.29	LWR 4547	L	23	
19.31	SWP 5301	L	28	
21.19	SWP 5320	L	30	
21.22	LWR 4561	L	25	
21.24	SWP 5321	L	50	12.03 ± .03
21.28	LWR 4562	L	37	
21.31	SWP 5322	L	30	
23.03	SWP 5335	L	30	
23.06	LWR 4567	L	25	
23.08	SWP 5336	L	30	
23.10	LWR 4568	L	25	12.00 ± .03
23.12	SWP 5337	L	30	
23.15	LWR 4569	L	25	
23.30	SWP 5338	L	30	
25.03	SWP 5348	L	30	
25.05	LWR 4591	L	25	
25.07	SWP 5349	L	25	12.02 ± .03
25.09	LWR 4592	L	25	
25.12	SWP 5350	L	50	
25.15	LWR 4593	L	25	
31.65	SWP 5414 (+)	L	30	
Jun 01.04	LWR 4658	L	25	
01.07	SWP 5421	L	25	
01.10	LWR 4659	L	25	
01.12	SWP 5422	L	25	
01.14	LWR 4660	L	25	
01.16	SWP 5423	L	25	11.97 ± .03
01.18	LWR 4661	L	25	
01.20	SWP 5424	L	25	
01.22	LWR 4662	L	25	
01.24	SWP 5425	L	25.5	
01.26	LWR 4663	L	25	

Date	Image	Ap	Exp time (min)	m_{FES}
1979				
Aug 07.77	SWP 6103	L	25	
07.80	LWR 5288	L	25	
07.82	SWP 6104	L	50	
07.86	LWR 5289	L	25	
07.88	SWP 6105	L	25	
07.91	LWR 5290	L	25	12.12 ± .03
07.93	SWP 6106	L	50	
07.97	LWR 5291	L	25	
07.99	SWP 6107	L	25	
08.01	LWR 5292	L	25	
08.03	SWP 6108	L	25	
08.05	LWR 5293	L	25	
Dec 07.79	LWR 6325(+)(x)	L	3x25	
07.85	SWP 7338(+)(x)	L	3x25	
07.93	LWR 6326(+)(x)	L	3x15	
07.97	SWP 7339(+)(x)	L	3x15	
12.59	SWP 7378	S	50	
12.63	SWP 7378	L	25	
12.65	LWR 6370	L	50	12.05 ± .03
12.69	SWP 7379	L	25	
12.71	SWP 7379	S	42	
13.45	SWP 7387	L	25	
13.47	LWR 6378	L	25	
13.49	SWP 7388	L	25	
13.51	LWR 6379	L	25	12.06 ± .03
13.54	SWP 7389	L	25	
13.56	LWR 6380	L	25	
13.58	SWP 7390	L	25	
13.98	SWP 7394(+)	L	15	
1980				
Jan 01.35	SWP 7517	L	25	
01.37	LWR 6509	L	25	
01.39	SWP 7518	L	25	12.08 ± .03
01.41	LWR 6510	L	25	
01.43	SWP 7519	L	25	
01.45	SWP 7519	S	50	
Mar 01.42	SWP 8098	L	25	
01.44	LWR 7065	L	25	12.08 ± .03
01.46	SWP 8099	L	43	
04.20	LWR 7095	L	25	
04.22	SWP 8161	L	25	12.08 ± .03
04.82	SWP 8163(+)	L	25	
06.19	LWR 7105	L	25	
06.21	SWP 8176	L	25	12.08 ± .03

Date	Image	Ap	Exp time (min)	m_{FES}
1980				
Apr 21.13	SWP 8795	L	25	
21.15	SWP 8795	S	25	
21.17	LWR 7570	L	25	12.12 ± .03
21.20	SWP 8796	L	37.5	
21.22	LWR 7571	L	37.5	
May 15.00	SWP 9000	L	40	
15.03	LWR 7758	L	25	12.01 ± .03
19.21	SWP 9050	L	25	
19.23	LWR 7797	L	25	
19.25	SWP 9051	L	25	12.04 ± .03
19.27	LWR 7798	L	25	
19.29	SWP 9052	L	47	

used the standard processing system (*IUESIPS*), but with an improved background determination; for the SWP images, we adopted a procedure used by Snijders (1980) to correct an error in the intensity transfer function, which seriously affected all images, conventionally reduced between 1978 July and 1979 August.

The few small-aperture spectra were corrected for a transmission factor estimated either from the ratio of the fluxes through the small and large apertures on the same day, or, lacking the large aperture exposure, from the normalization of the strength of the C III] + Si III] λ1900 emission feature by reference to other epochs as discussed in Paper I. In the latter case (1978 June 17 and October 31; see also Paper I for the 1978 May spectra) the absolute flux scale is of lower accuracy, and the continuum values are reported in brackets both in Table 3 and in the figures.

Because of a technical failure, the effective exposure time of the large aperture image SWP 5298 (1979 May 19) could not be properly measured, and the absolute flux scale of the extracted spectrum was normalized to that of the other five SWP images obtained on the same day.

Further details of the data reduction, and an estimate of the photometric accuracy and repeatability are given in Paper 1.

3 Measurements of the ultraviolet continuum

The choice of the wavelength intervals representing the continuum distribution was discussed in Paper I. Shortward of λ2000 two alternatives were considered – a 'low' and a 'high' continuum – and the former was argued to be more plausible. In this paper we shall describe only the 'low' continuum, and the ten intervals used are listed in Table 2.

First we intercompared the continua from spectra taken during the same shift of eight hours (see Table 1) to look for variations on this scale. The standard deviation from the mean for each of the 10 continuum points was calculated for these nearly simultaneous spectra: 3–5 per cent. We regard this as our best estimate of the random errors typically affecting the measurements based on a single exposure of good quality; seriously under- or over-exposed images, or data affected by image faults (1979 May 4) can have substantially larger errors (Table 3). Within an upper limit of five per cent we find no evidence for variations on a time-scale of hours.

Fig. 1 shows the $\log f_\upsilon - \log \upsilon$ plots of the continua measured on those days when large-aperture images were obtained both at short and long wavelengths. The continuum appears

Table 2. Spectral intervals used to estimate the continuum.

Central wavelength (Å)	Wavelength range (Å)
3020	40
2902.5	35
2705	30
2675	30
2410	20
2225	50
2165	70
2055	150
1705	10
1455	30

Table 3. Parameters of the ultraviolet continuum.

Date	f_{2500} 10^{-26} erg cm^{-2} s^{-1} Hz^{-1}	α_{LW}	f_{1455}	Δf_{1455} 10^{-26} erg cm^{-2} s^{-1} Hz^{-1}	Δf^c_{1455}
1978 Feb 28			13.4±1.0		
Apr 16-17	21.8±1.0	- 1.26±0.20	15.8±0.5	5.3±0.9	2.6±1.7
May 8-12	(23.5±0.6)	- 1.95±0.16	(15.1±0.7)	(6.9±1.0)	(6.1±1.8)
Jun 17			(11.8±0.6)		
Jul 24	16.7±0.4	- 1.84±0.16	10.9±0.3	4.7±0.6	3.8±1.1
Aug 2			9.5±0.5		
Oct 19	18.8±0.4	- 1.91±0.16	9.6±0.3	2.9±0.7	0.9±1.2
Oct 31	(11.3±0.4)	- 2.10±0.16	(4.3±0.2)	(0.7±0.4)	(<0.6)
Dec 9	15.2±0.4	- 1.84±0.16	8.3±0.3	2.7±0.6	1.1±1.1
1979 Jan 21	11.0±0.4	- 2.17±0.16	5.4±0.2	1.9±0.4	1.1±0.7
May 3	10.8±0.4	- 2.80±0.25	8.1±0.3	5.7±0.4	7.2±0.8
May 4			7.0±1.0		
May 19	17.7±0.2	- 1.69±0.08	12.5±0.4	5.5±0.5	4.4±0.8
May 21	19.4±0.3	- 1.47±0.16	13.6±0.4	4.9±0.9	2.8±1.6
May 23	19.0±0.4	- 1.77±0.11	13.1±0.4	5.8±0.6	4.8±1.1
May 25	20.0±0.3	- 1.60±0.11	13.7±0.4	5.3±0.7	3.5±1.2
May 31			13.6±0.6		
Jun 1	20.4±0.2	- 1.61±0.08	13.6±0.4	5.1±0.6	3.2±1.0
Aug 7-8	11.9±0.2	- 2.46±0.08	8.9±0.3	5.8±0.3	7.0±0.5
Dec 7	16.0±0.4	- 1.97±0.16	11.2±0.3	5.7±0.5	5.6±1.2
Dec 12	13.5±0.4	- 2.37±0.16	8.7±0.3	4.9±0.4	5.2±0.8
Dec 13.5	13.5±0.3	- 2.54±0.11	8.7±0.4	5.2±0.4	6.0±0.6
Dec 13.9			9.9±0.5		
1980 Jan 1	13.3±0.4	- 2.43±0.20	8.5±0.3	4.9±0.5	5.4±0.9
Mar 1	11.0±0.4	- 2.78±0.16	7.2±0.3	4.7±0.4	5.8±0.5
Mar 4.2	11.2±0.4	- 2.82±0.16	7.8±0.4	5.6±0.4	7.0±0.6
Mar 4.8			8.2±0.4		
Mar 6	12.9±0.4	- 2.53±0.16	9.3±0.5	6.0±0.5	7.1±0.8
Apr 21	6.5±0.4	- 2.73±0.25	2.6±0.2	1.1±0.3	0.8±0.5
May 15	14.8±0.4	- 2.11±0.15	12.7±0.4	8.0±0.6	9.3±1.0
May 19	17.9±0.5	- 1.52±0.15	12.4±0.4	4.6±0.8	2.8±1.4

to vary both in intensity and in shape, thus a description of its variability may require more than one parameter. The shape is generally consistent with that discussed in Paper I, namely that at long wavelengths the points can be reasonably well fitted by a power law, whose extrapolation falls below the flux measured at short wavelengths. In Paper I reddening corrections for various values of $E(B-V)$ were applied, but none would suppress the excess at short wavelengths. Hence it was suggested that the ultraviolet continuum is made up of two components, one dominating at the long, the other at the short wavelengths. Following Paper I we shall call them the long and the short wavelength components, and describe the continuum in terms of three parameters: the normalization and the frequency spectral index of power law, $f_\upsilon \propto \upsilon^{\alpha_{LW}}$, fitted through the points longward of λ2200 and the excess above this fit at λ1455.

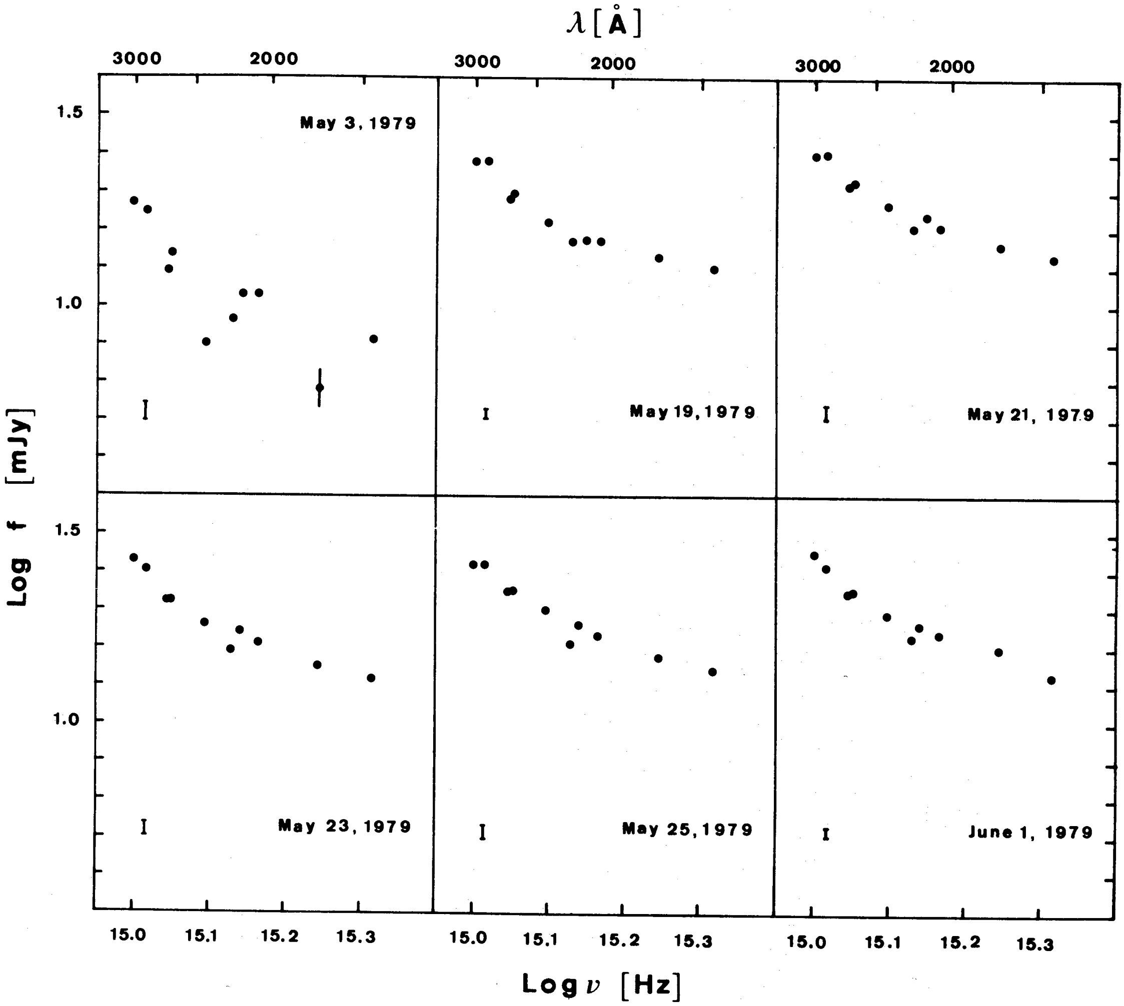

Figure 1(a). Ultraviolet continuum energy distributions for NGC 4151. A typical error bar is given in the lower left corner of each plot.

The only difference from Paper I is that the two points representing the intervals λλ 1980–2130 and λλ2130–2200 have been excluded from the fit, because of their peculiar behaviour. In all the continuum distributions shown in Fig. 1 (with the exception of 1978 April 16), these two points lie systematically above the best-fit straight line through the six points longward of λ2200. Curiously, this peculiarity did not appear in the 1978 spectra (see Paper I). The origin of this 'excess' around λ2100 is not clear, and some possible explanations are discussed in the appendix. Here we note that it prevents a reliable estimate of the λ2200 extinction feature. In this paper we shall still use $E(B-V)=0.05$, the value adopted in Paper I, but clearly the reddening correction is more uncertain than was thought before.

The continuum measurements, including the few presented in Paper I, are described in Table 3 by means of the following quantities: the flux at λ2500, f_{2500}; the frequency spectral index $\alpha_{\rm LW}$, obtained from the fit longward of λ2200; the flux measured at λ1455, f_{1455}; and the excess $\Delta f_{1455}=f_{1455}-f_{1455}^{\rm ext}$ above the extrapolations of the fit. When a reddening correction of the form given by Seaton (1979) is applied, with $E(B-V)=0.05$, one finds: $f_{2500}^{\rm c}=1.42 f_{2500}$, $\alpha_{\rm LW}^{\rm c}=\alpha_{\rm LW}+0.61$ and $f_{1455}^{\rm c}=1.47 f_{1455}$. The reddening corrected excess $\Delta f_{1455}^{\rm c}$ also is given in the Table.

In the following we shall tentatively regard f_{2500} and $\alpha_{\rm LW}$ as representing the strength and spectral index of the long wavelength component, and Δf_{1455} as a measure of the strength of

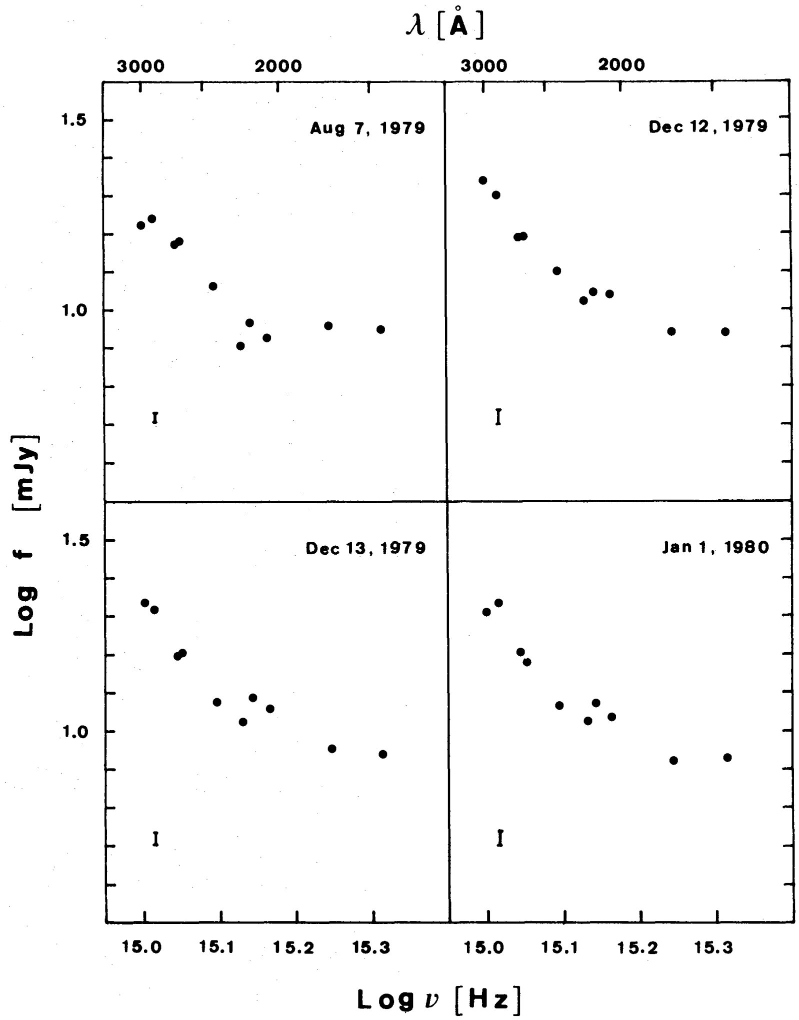

Figure 1(b). Same as Fig. 1(a).

the short wavelength component. This rough decomposition obviously is subject to the uncertainty in the weaker component in the wavelength range where the other dominates. It is noteworthy that on some occasions (e.g. 1979 May 3), the two points at λλ1705 and 1455 define a slope such that its extrapolation to longer wavelengths gives a negligible contribution to the points used to estimate f_{2500} and α_{LW}. Of course, there is no guarantee that this is always the case, hence any conclusion concerning the behaviour of the two components taken independently must be considered with caution.

4 Temporal behaviour of the ultraviolet continuum

4.1 LIGHT CURVES

The quantities f_{2500}, f_{1455}, Δf_{1455} and Δf^{c}_{1455} are plotted as a function of time in Fig. 2. The broken horizontal lines represent a reference value, defined as the straight mean of all the points in the light curves. Occasionally we shall call 'high' and 'low' states the points respectively above and below this reference line.

The distributions of f_{2500} and f_{1455} on the whole look very similar. The high and low states are generally simultaneous at the two wavelengths, and are all within ± 50 per cent of the mean, with the exception of 1980 April 21, a low state 75 per cent below the average. The standard deviation from the mean is 26 per cent in f_{2500} and 30 per cent in f_{1455}.

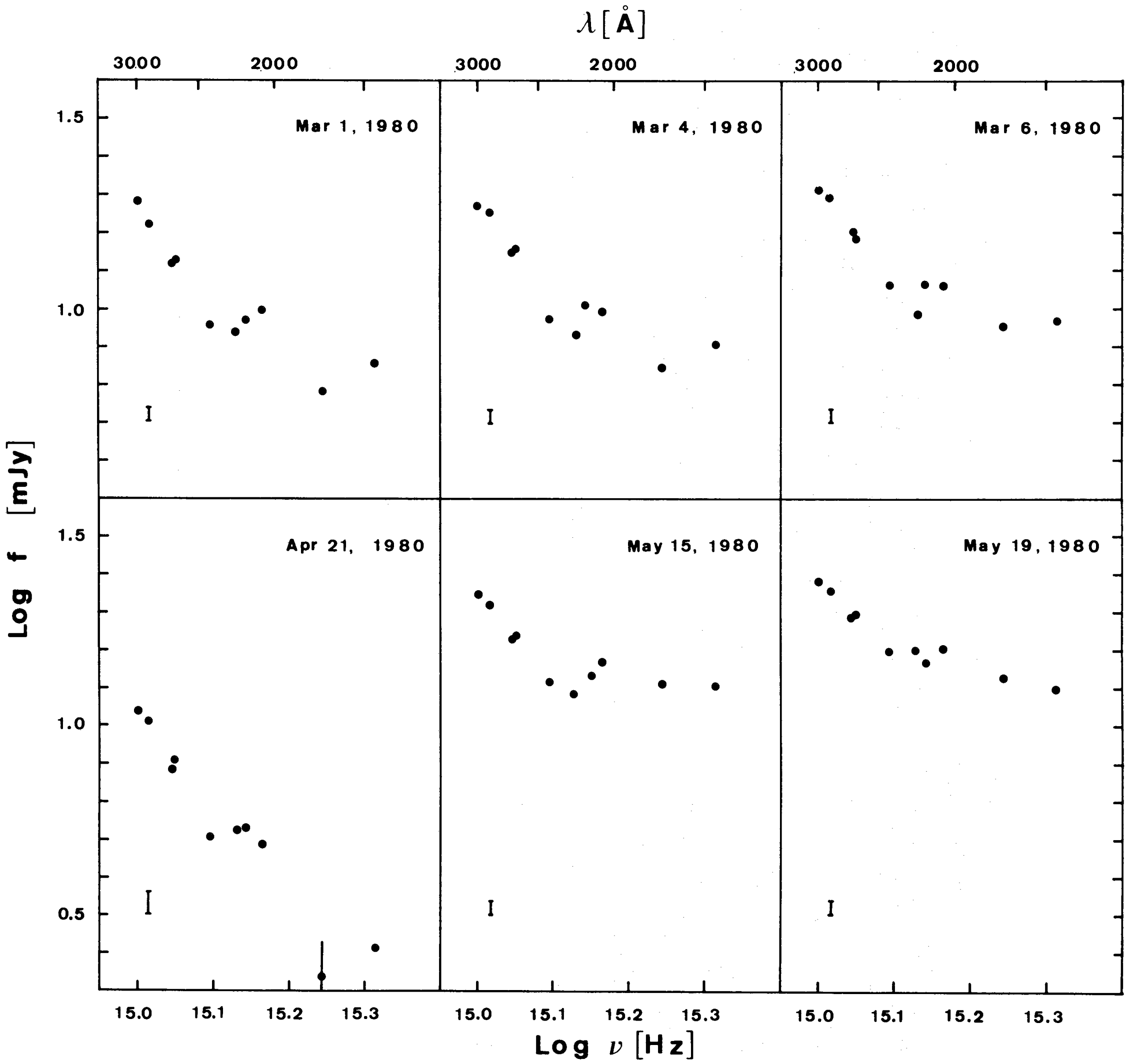

Figure 1(c). Same as Fig. 1(a).

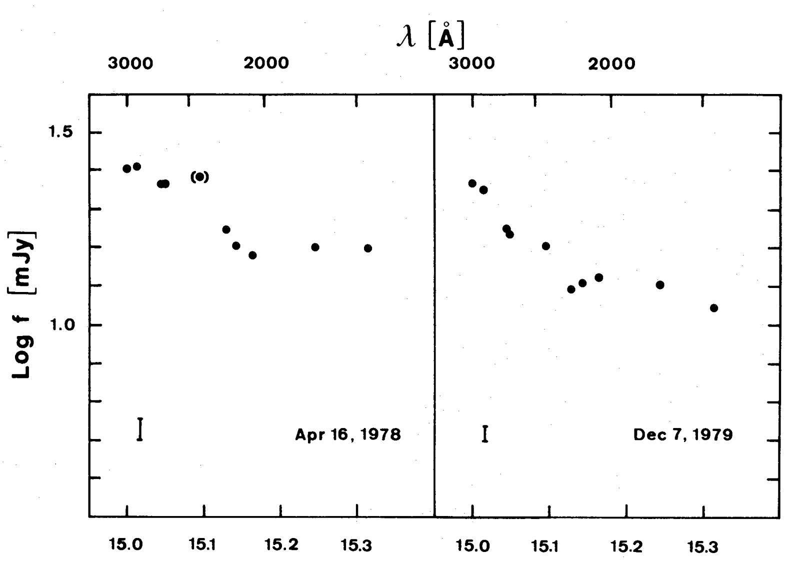

Figure 1(d). Same as Fig. 1(a). The point in brackets in the 1978 April 16 spectrum was excluded from the long wavelength fit described in the text. These two distributions are from spectra retrieved from the data bank.

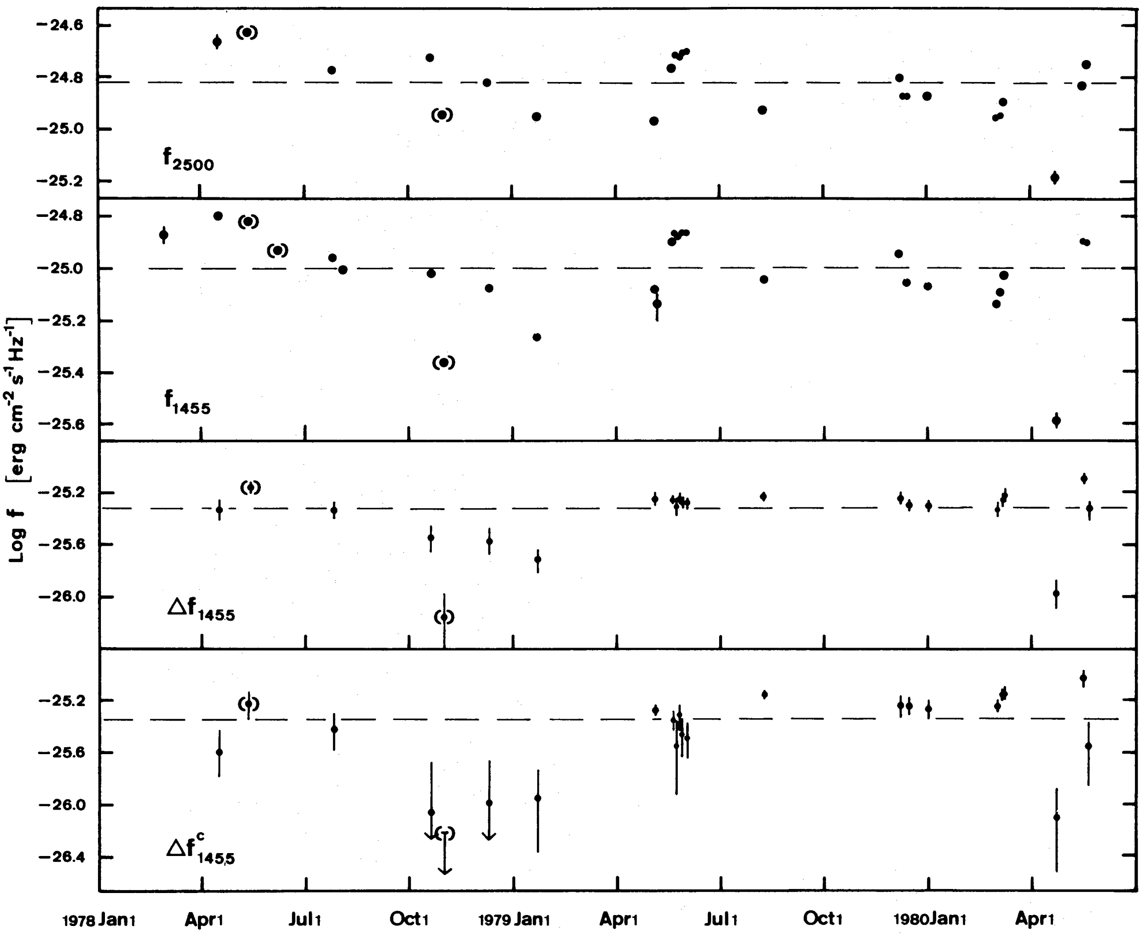

Figure 2. Light curves of the ultraviolet continuum at long and short wavelengths. The excess at short wavelengths is plotted before and after correction for reddening with $E(B-V)=0.05$. Note that the vertical scale in the upper two panels is double that in the other two. The points in brackets are from spectra taken through the small aperture, and their absolute calibration is uncertain. The broken horizontal lines represent a straight mean of the points in the plots.

On the contrary, a detailed comparison of the light curves of f_{2500} and Δf_{1455} ($E(B-V)=0.0$) shows little correspondence in the behaviour of the two quantities; this was already noted in Paper I. Before discussing the behaviour of Δf_{1455} and Δf^c_{1455}, we shall first consider the behaviour of α_{LW}, the other parameter we have chosen to describe the continuum.

The spectral index α_{LW} undergoes large variations, between minimum and maximum recorded values of -2.8 and -1.3. A very striking result is that the variations in α_{LW}, as judged from Fig. 3, are closely correlated with those of f_{2500}, in the sense that the spectrum hardens when the flux increases. This correlation is shown in Fig. 4. A linear regression analysis to the large aperture data yields a highly significant correlation coefficient of 0.91.

When the excess at λ1455 over the extrapolation of this power law is calculated without regard to reddening, it is found to be nearly constant from 1979 May 3 to 1980 March 6, independent of f_{2500} (or α_{LW}). We find for this period $4.5 \leqslant \Delta f_{1455} < 6.0$ mJy. Between 1978 October and 1979 January the excess was low: $\Delta f_{1455} < 3$ mJy. On 1980 April 21 the fluxes were the lowest observed so far and the excess was only 1.1 mJy. The single reliable measurement of an excess larger than 6 mJy is the very next observation on 1980 May 15: $\Delta f_{1455} = 8.0 \pm 0.6$ mJy. The overall mean excess is 4.8 mJy with standard deviation 1.5 mJy. The lack of any dependence of Δf_{1455} on f_{2500} for most of the data is evident in the top part of Fig. 5.

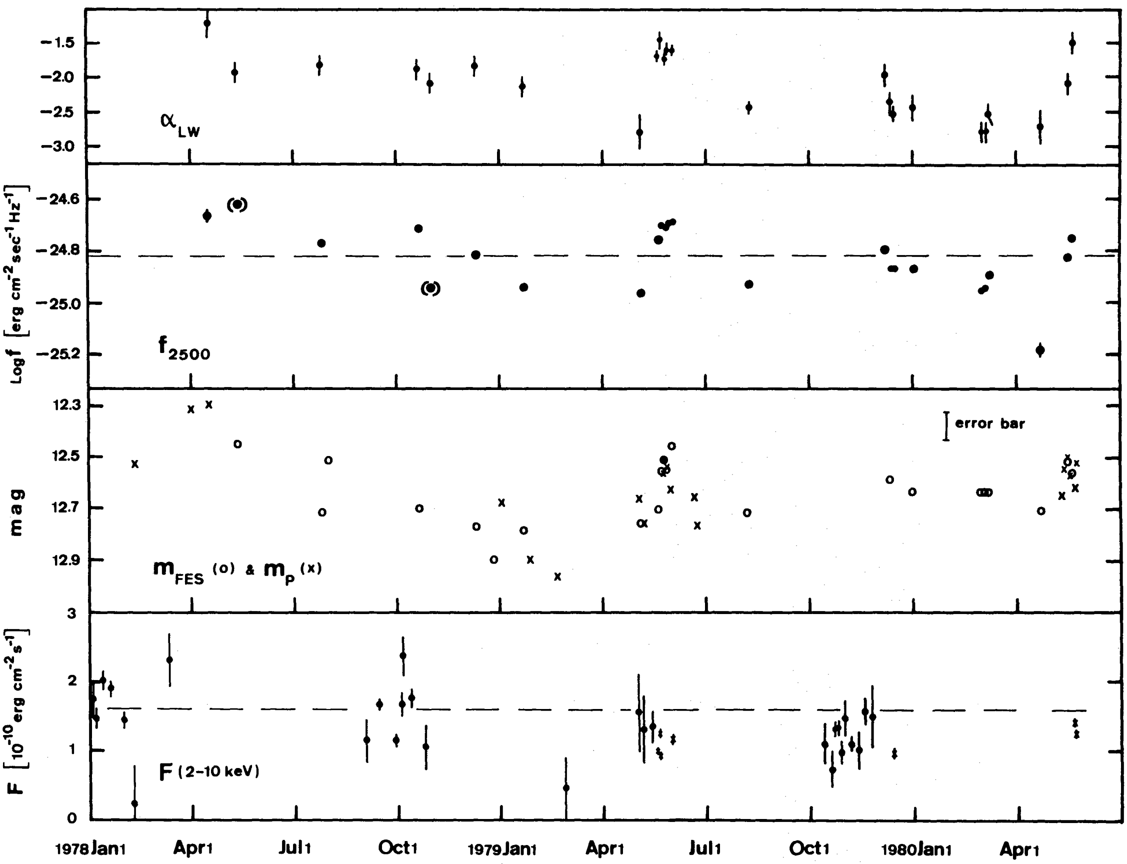

Figure 3. Light curve of the ultraviolet continuum at long wavelengths compared with: variations in the best fit power-law slope at long wavelengths (first panel); variations in the optical magnitude (third panel, only a typical error bar is shown); variations in the X-ray energy flux (fourth panel; symbols: dots = *Ariel V* SSI measurements, crosses = *HEAO-B* MPC measurements; the broken line represents the weighted mean of all SSI measurements over the years 1974–79).

However, if we make and extrapolate the fit to the long wavelength data using a power law reddened by $E(B-V)=0.05$, we find that the corrected short wavelength excess, Δf^c_{1455}, shows the rather different behaviour, illustrated in the lower part of Fig. 5. In this, probably more realistic, case we obtain a loose anticorrelation between Δf^c_{1455} and f_{2500} with the same exceptions to the main trend as before: the data from 1978 October to 1979 January and from 1980 April 21 to 1980 May 15. There is a suggestion that the short wavelength excess at the epochs when it is anomalously low has a constant value near $\Delta f^c_{1455}=1$ mJy.

The difference in appearance of the two parts of Fig. 5 and the different physical conclusions that might be drawn from them underline the call for caution at the end of Section 3 concerning the interpretation of our decomposition of the continuum energy distributions. In the broadest terms, however, our results in this section show a continuum, variable in both shape and intensity, which can be specified by a single parameter except for a few anomalous epochs when the flux at λ1455 is discrepant. Certainly the flux variations at different wavelengths are not simply proportional to each other. On the other hand the fact that there is an excellent correlation between f_{2500} and α_{LW}, which holds up even when the λ1455 excess is in an 'anomalous' state, suggests the existence of an independent short wave component with a separate physical origin. The weakness of the excess on 1978 October 19, when the C IV emission line reached the greatest strength so far observed, argues against an interpretation of the excess in terms of unknown or unsuspected emission lines and

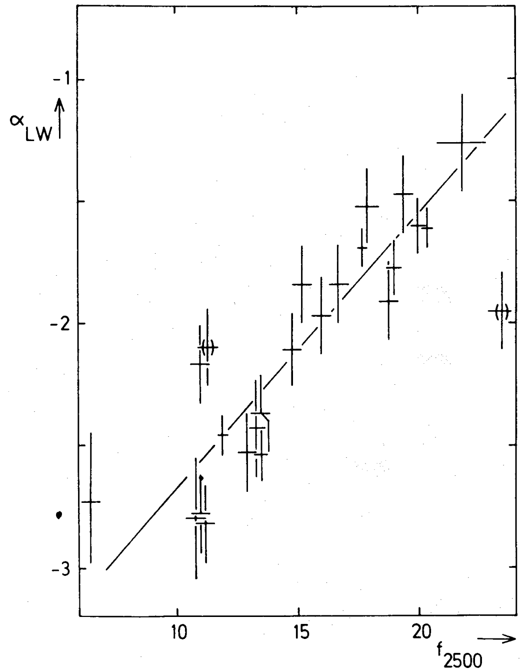

Figure 4. Showing the correlation between α_{LW} and f_{2500}. The small aperture data are given in brackets and are excluded from the linear least squares fit to the data.

supports its adoption as a continuum indicator. We return to the discussion of this component in Section 7.

4.2 ARE THE OBSERVED VARIATIONS INTRINSIC TO THE CONTINUUM OR DUE TO A VARIABLE EXTINCTION?

The type of correlation found between f_{2500} and α_{LW} calls for a discussion of the possibility that the intensity variations might have an extrinsic origin. Assuming an intrinsically constant

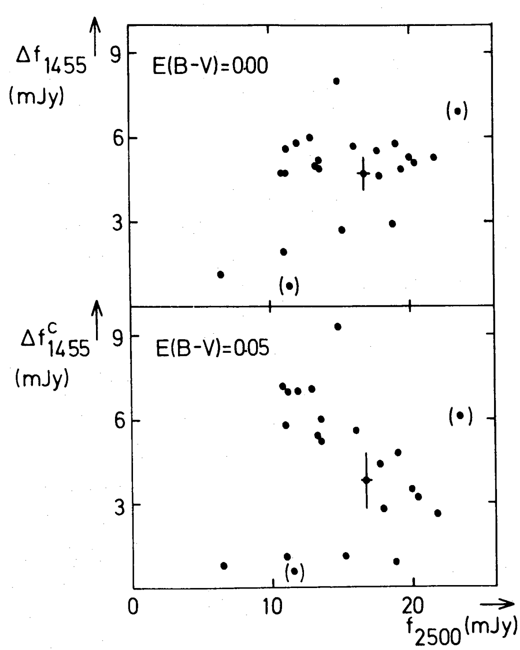

Figure 5. Top – dependence of Δf_{1455} on f_{2500} for $E(B-V)$ = 0.0. The two small aperture points are shown in brackets. To avoid confusion only one sample error bar is given; below – the same for Δf^{c}_{1455} and f_{2500} for $E(B-V)$ = 0.05.

continuum and a variable $E(B-V)$, for a wavelength dependence of the extinction as given by Seaton (1979), the expected correlation between f_{2500} and α_{LW} is surprisingly close to that observed. Furthermore the variations in f_{1455} relative to those in f_{2500} then also agree rather well with expectation except, however, for a few cases, namely when Δf_{1455} appears, as described above, either exceptionally low or high. The implication would then be that inside the nucleus of NGC 4151 there is a screen of dust intercepting the continuum, whose optical thickness varies substantially on time-scales (see next paragraph) which can be as short as five days.

There are, however, arguments, relying upon the variations observed to occur in the emission and absorption lines (Paper I) and in the near infrared continuum, which lead us to favour the view that the ultraviolet continuum variations are intrinsic.

(i) As already shown in Paper I, and as will be described and discussed in more detail using the new observations in forthcoming papers, the variations in the broad emission lines and in the absorption lines are correlated with the continuum in a way which is most reasonably explained in the framework of a photoionization model with a variable continuum. To reconcile the observed correlations with an intrinsically constant continuum output we have considered two possibilities, neither of which look very realistic. The first is that a variable dust screen surrounds the continuum source and is situated between this source and the broad line emitting gas. The distance of the screen from the continuum source would have to be less than 15 light-days from the lag between continuum and emission line variations – (Ulrich *et al.* in preparation). This seems too small for the dust grains to survive evaporation since an equilibrium temperature of 1500 K is obtained at a distance of $\gtrsim$ one light-month for a continuum luminosity of $1.5 \times 10^{10} L_\odot$ (*cf.* Rieke & Lebofsky 1981).

The second possibility is that the dust is mixed with the broad line gas and that its abundance changes coherently over the whole region, in such a way as to influence the continuum reaching the observer and the gas responsible for the absorption lines, and at the same time to mimic on the intensity of the emission lines the effects that one would attribute to the observed changes of the continuum. A variant of this picture is that the dust is not associated with the emission line gas, and should be located just outside the broad line region and inside the region where the gas responsible for the absorption lines is distributed.

(ii) In the near-infrared (1.6–2.2 μm) variations occur whose amplitudes are nearly comparable to those found in the optical and in the ultraviolet (Penston *et al.* 1974; Lebofsky & Rieke 1980; Rieke & Lebofsky 1981). Since the near-infrared is most likely due to reradiation by dust grains, its variations are explained in terms of changes in the optical-ultraviolet continuum responsible for the heating of the grains. This interpretation is supported by the correlation found between the infrared and the optical variations, in fact some evidence exists that the infrared lags behind the optical, as one would expect on the basis of a self-consistent model. If, alternatively, the infrared variations were merely due to changes in the amount of dust, then one would rather expect an anticorrelation with those seen in the optical.

In the following we shall therefore regard the continuum variations as intrinsic to the continuum source.

4.3 TIME-SCALE OF VARIABILITY

In Section 3, it is already reported that no significant changes were found among spectra taken during the same observing shift, thus implying as far as our evidence goes, that variations in the continuum were smaller than five per cent on a time-scale of a few ($\lesssim 8$) hours. On ten occasions *IUE* observations were made with intervals less than three days

(Table 1). These are grouped into six 'runs' of data spanning between one and 30 days. There are quite significant increases or decreases in flux during five of these six cases. In three runs (1979 May 3–June 1; 1980 March 1–6; 1981 April 21–May 19) the continuum brightened; in particular during 1979 May and 1980 April–May large outbursts took place. On the other two occasions (1978 October 19–31 and 1979 December 7–13) the continuum faded; conspicuously in the former case.

While in none of these five cases can we be sure that our data define the most rapid changes that occurred, we can give a lower limit to the rate of change by estimating an indicative time-scale from the change in flux between adjacent observations. We define this time as

$$\tau = \Delta t\, f_{\min}/(f_{\max} - f_{\min})$$

where Δt is the interval between the two observations and $f_{\max}$ and $f_{\min}$ are respectively the larger and smaller fluxes at those two times, and summarize in Table 4 the shortest of these during each run at both λ2500 and λ1455. These times correspond to the time in which the flux would increase or decrease by a factor of 2 if the same rate of change continued outside interval between data points, hence we shall call them 'two-folding time-scales'. These time-scales turn out to be similar for intensity increases and decreases, and lie between five and 30 days. The significant difference in τ at the two wavelengths found on two occasions can be interpreted as further evidence that variations in the two components of the continuum are not proportional to each other.

A much shorter rise time, of the order of one day, was tentatively suggested by Boksenberg *et al.* (1978) from comparison of a SW spectrum taken on 1978 February 11 (during the *IUE* Commissioning Phase) with the previous day's rocket measurement by Davidson & Hartig (1978), when a possible three-fold increase was indicated. The large changes between the rocket spectrum of 1978 February 10 and the well-exposed *IUE* spectrum of February 28 are similar to the changes we observed in the outburst between 1979 May 3 and 21 in respect of the absolute flux levels, continuum slope and differential changes in absorption lines from ions of high and low ionization levels. However, in 1978 we additionally have the low quality *IUE* SW spectrum of February 11 which indicated that the doubling of the continuum flux took place in about one day instead of $\lesssim$ 20 days as in 1979 May. Since we have found no further evidence of doubling times so short, there remains the suspicion that an error in the rather uncertain estimated continuum for 1978 February 11 was responsible for that result.

Our data suggest that variations with typical two-folding time-scales of five to 30 days are common and that such outbursts cause the rather erratic behaviour of the light curves we

Table 4. Variability in the ultraviolet: Doubling time-scales.

Epoch	Increase	Decrease	τ(2500 Å) (day)	τ(1455 Å) (day)
1978 Feb 10–28	X			$\lesssim 15^{\star}$
Oct 19–30		X	(16 ± 1.5)	(9 ± 0.5)
1979 May 3–21	X		23 ± 1.5	26 ± 2.5
Dec 7–12		X	27 ± 6	17 ± 3
1980 Mar 4–6	X		13 ± 5	10 ± 4
Apr 21–May 15	X		19 ± 2	6 ± 0.5
May 15–19			19 ± 4	no var.

★Estimated from the results of Davidsen & Hartig (1978) and Boksenberg *et al.* (1978) as modified in Paper I.

have constructed. Because of their occurrence a more systematic and regular monitoring is needed to establish whether a long-term variability is also present and in particular to look for an underlying periodicity. This would also provide us with detailed information on the structure and amplitude distribution of each isolated outburst. It would be interesting to discover, for example, whether the behaviour during the event in 1979 May, when the flux remained near its maximum for at least 12 days, is typical.

5 Optical observations

The *IUE* Fine Error Sensor provides a measurement of the optical light around λ4800, at the same time as the ultraviolet observations. The magnitudes m_{FES} are given in Table 1, where the errors quoted are typically smaller than in Paper 1 as a result of a critical re-examination of the FES data. In addition, photographic magnitudes m_{pg} have been obtained with the 26-inch Thompson refractor at the RGO (see Cannon, Penston & Brett 1971 for the technique used), which partly overlap with the ultraviolet measurements. These magnitudes are measured through an aperture of about 3 arcsec. Comparing m_{pg} and m_{FES} values measured on the same day, we find an extra constant source equivalent to 13.07 mag is included in the FES magnitudes, which we attribute primarily to starlight contamination from the surrounding galaxy through the larger FES aperture. It also conceals the difference in photometric systems which is small (~ 0.2 mag). Both m_{pg} and m_{FES}, the latter corrected in this empirical way, are plotted in Fig. 3, where an error bar of 0.05 mag is assigned to each point.

There is no obviously repeatable periodic behaviour in the optical light curve; nor have any confirmed periods been found in the light curves of this or other active nuclei. Because the optical light curve contains the most observations (covering 45 different days in the period 1978 June–1980 May) it was felt worthwhile to quantify this statement by analysing the power spectrum of the combined FES and photographic magnitudes. It was found that there is no significant peak in this power spectrum in the period range 10 to 100 days, the largest peak corresponding to an amplitude of 0.06 mag.

The optical light curve shows on the whole a fairly similar behaviour to that at λ2500, thus supporting the conclusion reached in Paper I that the long wavelength ultraviolet flux is probably merely an extrapolation of the optical continuum. The amplitude of the variations is somewhat smaller in the optical than in the ultraviolet. The difference could be due to a residual starlight contamination or to the correlation between the slope and the strength of the continuum which we have found in the ultraviolet, or both. One can also note some subtle differences in the relative position of the optical magnitudes and the λ2500 flux along their respective light curves, the most conspicuous occurring on 1980 April 21, when m_{FES} was close to its average value, while f_{2500} was at the lowest level recorded. We believe their significance is marginal, and that one should await more accurate simultaneous optical measurements, possibly including those suitable for determining the slope of the continuum, before any conclusion is drawn.

6 X-ray observations

6.1 *ARIEL V* OBSERVATIONS

An extensive monitoring of the 2–10 keV flux carried out with the Sky Survey Instrument (SSI) on the *Ariel V* satellite (Lawrence 1980) showed an erratic behaviour, with variations up to a factor 2 from the mean value. Prominent features are flare-like events, characterized by rise times of the order of half a day and decay times of the order of 2–4 day. Spectral measurements (Ives, Sanford & Penston 1976; Barr *et al.* 1977; Mushotzky *et al.* 1978, 1980) have shown that the medium energy X-ray continuum can be described by a power law with a photoelectric cut-off. The energy spectral index α_X, $dF_E/dE \propto E^{\alpha_X}$ remains practically constant, even during an outburst (Mushotzky *et al.* 1978) and equal to -0.45 ± 0.10, while the column density N_H responsible for the cut-off varies on a time-scale of months in the range 3.5 to $20 \times 10^{22}\,cm^{-2}$. For an otherwise constant spectrum, a change in N_H alone from the lowest to the highest of the values recorded implies a decrease of the 2–10 keV flux by 60 per cent.

The last panel of Fig. 3 contains the SSI measurements during the period 1978–79. The SSI count rates have been converted into an energy flux using the factor $1\,count\,s^{-1} = 5.0 \times 10^{-11}\,erg\,cm^{-2}\,s^{-1}$, which applies for a spectrum with $\alpha_X = -0.5$ and a column density $N_H = 8 \times 10^{22}\,cm^{-2}$. The weighted mean of all SSI measurements over the years 1974–79 is represented by the broken horizontal line, and the standard deviation about the mean is 35 per cent, similar to that found in the ultraviolet.

6.2 *EINSTEIN OBSERVATORY* OBSERVATIONS

Some of our *IUE* measurements were timed to be quasi-simultaneous with observations done with the *Einstein Observatory*. The latter consisted of long exposures performed either with the Imaging Proportional Counter or with the High Resolution Imager, both instruments being sensitive in the soft X-rays. During the exposures, counts were recorded also from the Monitor Proportional Counter, which is sensitive in the range 2–20 keV and has a limited spectral resolution (Giacconi *et al.* 1979; Grindlay *et al.* 1980); these counts were used to obtain the 2–10 keV fluxes presented in this paper.

At the sensitivity required here, the elimination of the background from the MPC counts is unreliable above 10 keV, so we used only the counts below this energy. Furthermore, we rejected several segments of the exposures when a residual background contamination was clearly present in the net counts between 6 and 10 keV. The net count rates from the remaining segments are given in Table 5, along with the flux and the absorbing column N_H

Table 5. Monitor Proportional Counter data from observations with the *Einstein Observatory*.

Date	Count rate (2–10 keV) (sec^{-1})	Flux (2–10 keV) ($10^{-11}\,erg\,cm^{-2}\,s^{-1}$)	N_H ($10^{22}\,cm^{-2}$)
1979			
May 19.00–19.01	4.31 ± 0.19	9.88 ± 0.49	
19.40–19.48	5.04 ± 0.08	12.82 ± 0.64	
19.73–19.81	4.69 ± 0.08	12.31 ± 0.62	11.5 ± 3.0
20.25–20.26	4.44 ± 0.13	11.66 ± 0.58	
20.72–20.91	3.84 ± 0.09	9.32 ± 0.47	
May 31.19–31.41	4.55 ± 0.08	11.70 ± 0.58	$8.4^{+2.8}_{-2.3}$
Dec 13.43–13.50	3.99 ± 0.08	9.66 ± 0.48	$11.5^{+5.3}_{-3.0}$
1980			
May 20.15–20.30	5.97 ± 0.06	14.18 ± 0.71	$14.5^{+2.3}_{-2.0}$
20.89–20.96	5.17 ± 0.10	12.38 ± 0.62	

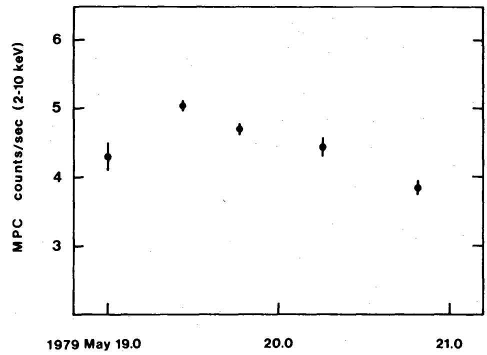

Figure 6. The small amplitude X-ray flare recorded with the Monitor Proportional Counter on *HEAO-B*.

estimated from the fit to the energy distribution of the counts. Because of the strong absorption, the spectral index is not as well determined, but the values obtained from the fit are all consistent with $\alpha_X = -0.5$. The errors quoted in Table 5 for the count rates are from counting statistics only, while those quoted for the fluxes include the uncertainties in the fit parameters.

On two occasions the measurements extend over one or two days, and they clearly show intraday variability. The clearest case (1979 May 19–20) is illustrated in Fig. 5; between the first and the second record, separated by 10 hours, the flux increased by 30 per cent, and then declined by the same amount in about 24 hours. The peak flux was 20 per cent less than the average SSI flux, so we would call this variation a mini-flare. In the other case (1980 May 20), the flux declined by 15 per cent in about 17 hours.

These measurements are plotted together with those from the SSI in Fig. 3.

6.3 COMPARISON BETWEEN THE TEMPORAL BEHAVIOUR IN THE ULTRAVIOLET AND IN X-RAYS

Although both the ultraviolet and the X-ray flux have an erratic behaviour, with standard deviations about the mean which are similar, the detailed temporal structure of their variations are strikingly different. The X-ray flares have a rise-time typically a factor 10 shorter than the shortest time-scale we have definitely found for large variations in the ultraviolet. Furthermore, while an X-ray flare is immediately followed by a rapid decay, in the 1979 May outburst the ultraviolet flux remained close to its maximum value for at least 12 days. Such differences in the temporal behaviour suggest that the spatial structures of the emission mechanisms operating in the two widely separated frequency bands are also quite different.

However, if the energy source is one and the same, one would expect some kind of association in time between the variations in the X-rays and in the ultraviolet. Because of the time-scales involved, an investigation of this property would require a systematic simultaneous monitoring at intervals of one or a few days over a period of months. The data we have collected so far are on the whole too fragmentary to fulfil this requirement, but fortunately the five SSI and MPC measurements made in 1979 May 1–31 overlap with the large ultraviolet outburst. No sign of a strong X-ray activity was recorded. In particular it is noteworthy that on May 19–20, when the ultraviolet flux reached the high intensity plateau, and on May 31, when it was still on the plateau, the X-ray flux remained below the average. We cannot exclude the possibility that a large X-ray flare occurred between these two dates, but we can at least exclude a simultaneous increase of the X-ray flux when a large energetic event occurred in the ultraviolet. The absence of a close correlation is possibly due to a time lag or lead between the ultraviolet and the X-ray variations, which may be of the order of a few days, if we happened to miss a large X-ray flare, or by more than 10 or 15 days otherwise.

7 Discussion and conclusions

7.1 IMMEDIATE DEDUCTIONS FROM THE DATA

The fastest ultraviolet variations we have so far detected have (two-folding) time-scales of five to 30 days and their immediate implication is that a major fraction of the ultraviolet continuum comes from a region smaller than 0.01 pc. In the case of the well-observed 1979 May outburst the total energy emitted in the ultraviolet was at least 3.10^{48} erg (assuming a distance of 10 Mpc).

The variations in the 2–10 keV X-rays have a similar standard deviation about the average flux to those in the ultraviolet, 30 per cent. Furthermore, the energy emitted in the ultraviolet outburst of 1979 May is comparable to that emitted in a large X-ray flare. However, there are striking differences in the temporal behaviour, the shortest time-scale observed being a factor of about 10 shorter in the X-rays than in the ultraviolet. Moreover, on the basis of the only extended overlap between the X-ray and ultraviolet monitoring which occurred during the 1979 May outburst, we conclude that the variations in the two bands are not closely associated in time. The implications are not only that the X-rays apparently come from a region about ten times smaller than the ultraviolet photons, but also that if the X-ray and the ultraviolet outbursts are manifestations of the same energetic events, there must be a time difference between their occurrence, which as far as our evidence goes, could be either a few or alternatively more than 10–15 day.

It is rather less certain exactly what can be deduced from the complex variations of the ultraviolet continuum discussed in Section 3 and illustrated in Figs 4 and 5. One relevant point, however, is the contribution at $\lambda 1455$ expected from the stellar content of NGC 4151. This is difficult to predict because the ultraviolet flux depends on the population of early-type stars which cannot be well established by optical observations alone and varies from galaxy to galaxy (e.g. Fosbury *et al.* 1981). Adopting, however, $B = 13.5$ for the magnitude of the stellar contribution within 5 arcsec of the nucleus (Penston *et al.* 1974) and the blue-to-ultraviolet colours of M87 (Bertola *et al.* 1980; Perola & Tarenghi 1980), one finds an expected contribution $f_{1455} = 0.3$ mJy, interestingly close, given the uncertainties, to the 1 mJy level of Δf^{c}_{1455} when NGC 4151 is in its anomalous state (Fig. 5).

The existence of this anomalous state is fairly well established, regardless of the way in which the continuum is actually decomposed, by the separation of the majority of points from those representing the anomalous state in both parts of Fig. 5. In all but one case this corresponds to a severe weakening or vanishing of any short wavelength excess. This is the type of phenomenon which is naturally explained by a partial or total occultation of the source of the normal short-wave excess. However, it is clear that other possibilities are not excluded.

7.2 COMPARISON WITH THEORETICAL MODELS

It is worth stressing some implications of our findings for the current theoretical models. In the framework of an accretion model (e.g. Rees 1979), Compton scattering of soft photons in a very hot ($\sim 10^9$ K) infalling gas can lead to a power-law continuum extending from the optical to the X-rays (for a simple model of this type, see Maraschi *et al.* 1979; for detailed calculation on this process see Sunyaev & Titarchuk 1980 and references therein). The slope of the power law depends on the optical depth, hence on the accretion rate, and the prediction is that the slope should become shallower when the luminosity increases. This is qualitatively in agreement with the correlation found between the slope and the strength of the continuum at long ultraviolet wavelengths. On the other hand, the bulk of the X-rays cannot be due to the same emission mechanism, since the change in slope would imply much larger variations in their intensity than is observed, and they should be also closely correlated with the ultraviolet variations. This suggests a model where the X-rays are emitted through a different process (for example, non-thermal or bremsstrahlung emission, see Rees 1979) dominating in the innermost regions of the accretion flow. In such a model it might be possible to accommodate a substantial lag between the X-ray and the optical–ultraviolet variations.

The excess at short ultraviolet wavelengths is reminiscent of the bump observed in the optical–ultraviolet spectrum of the quasar 3C 273 by Ulrich *et al.* (1980), who suggested the interpretation of thermal emission from gas around 10^5 K in an accretion flow. A thermal explanation for the short wavelength component in NGC 4151 was also proposed in Paper I. The long and short wavelength components could then be identified with the emission from two distinct phases in the accreting gas, and in a non-stationary situation one might perhaps explain the observed difference in their variations.

The small degree of polarization in the optical continuum observed by Thompson *et al.* (1979) and by Schmidt & Miller (1980) is an indication that at least part is of synchrotron origin. This brings us to the 'classical' interpretation of the continuum emission of active nuclei involving synchrotron and inverse Compton radiation from relativistic electrons, the first responsible mainly for the optical to ultraviolet continuum and the second for the X-ray emission. A model where the two processes operate in the same volume of space is excluded by the lack of temporal correlation. Cavaliere & Morrison (1980) proposed an inhomogeneous version of the model, where the electrons are continuously accelerated over an extended region: in the inner parts of this region the magnetic energy density is larger than the radiation density, so the synchrotron emission dominates; in the outer parts the situation is reversed, and the inverse Compton process takes over. An attractive feature of this version is that changes in the rate and spatial extent of the acceleration cause variations in the optical–ultraviolet and in the X-rays which are not necessarily well correlated in time. However, a serious difficulty is that one would expect the time-scales to be shorter in the ultraviolet than in the X-rays. A pure non-thermal model matching the properties of the NGC 4151 continuum still needs to be elaborated.

7.3 FUTURE WORK

The results presented show that in order to obtain a fully satisfactory picture of the 'dynamics' of the continuum from the optical to the X-rays further monitoring is needed. This should consist of simultaneous observations made at intervals of at most a few days over a period of a few months. This is the only way to check whether variations in different components of the continuum are associated but far from synchronous because of systematic time lags. Optical measurements should if possible be more accurate than those presented in this paper and also give the slope of the continuum. Simultaneous measurements of the optical polarization would be most valuable, to check whether the polarized flux varies together with the total optical–ultraviolet flux. If this were the case, it would represent strong evidence that the continuum is totally non-thermal in origin.

Finally, we recall that the infrared continuum also undergoes variations, which typically occur about one month later than those in the optical (Penston *et al.* 1974). The current interpretation of the infrared emission (e.g. Lebofsky & Rieke 1980) as due mainly to reradiation by dust requires a detailed balance between the energy outputs in the infrared and ultraviolet, that can only be checked by means of simultaneous and extended observations in the two bands.

Acknowledgments

It is a pleasure to acknowledge that both the European Space Agency and Science and Engineering Research Council selection committees supported the ultraviolet observations generously. We have also benefited from the observations of several other observers whose data have been retrieved. GCP and EGT thank B. Falconi and G. Sechi and acknowledge financial support from the CNR. J. Halpern and J. Grindlay are acknowledged for their work on the *Einstein Observatory* MPC software. The *Ariel V* project is funded by the SERC.

References

Barr, P., Ives, J. C., Sanford, P. W. & White, N. E., 1977. *Mon. Not. R. astr. Soc.*, **181**, 465.

Bertola, F., Cappaccioli, M., Holm, A. V. & Oke, J. B., 1980. *Astrophys. J.*, **237**, L65.

Boggess, A., Carr, F. A., Evans, D. C., Fischel, D., Freeman, H. R., Fueschel, C. F., Klinglesmith, D. A., Krueger, B. L., Longanecker, G. W., Moore, J. V., Pyle, E. J., Rebar, F., Sizemore, K. O., Sparks, W., Underhill, A. B., Vitagliano, H. D., West, D. K., Macchetto, F., Fitton, B., Barker, P. J., Dunford, E., Gondhalekar, P. M., Hall, J. E., Harrison, V. A. W., Oliver, M. B., Sandford, M. C. W., Vaughan, P. A., Ward, A. K., Anderson, B. E., Boksenberg, A., Coleman, C. I., Snijders, M. A. J. & Wilson, R., 1978. *Nature*, **275**, 372.

Boggess, A., Bohlin, R. C., Evans, D. C., Freeman, H. R., Gull, T. R., Heap, S. R., Klinglesmith, D. A., Holm, A. V., Perry, P. M., Schiffer, F. H., Turnrose, B. E., Wu, C. C., Lane, A. L., Linsky, J. L., Savage, B. D., Benvenuti, P., Cassatella, A., Clavel, J., Heck, A., Macchetto, F., Penston, M. V., Selvelli, P. L., Dunford, E., Gondhalekar, P., Oliver, M. B., Sandford, M. C. W., Stickland, D., Boksenberg, A., Coleman, C. I., Snijders, M. A. J. & Wilson, R. E., 1978. *Nature*, **275**, 377.

Boksenberg, A., Snijders, M. A. J., Wilson, R., Benvenuti, P., Clavel, J., Macchetto, F., Penston, M. V., Boggess, A., Gull, T. R., Gondhalekar, P., Lane, A. L., Turnrose, B., Wu, C. C., Burton, W. M., Smith, A., Bertola, F., Cappaccioli, M., Elvius, A. M., Fosbury, R., Tarenghi, M., Ulrich, M. H., Hackney, R. L., Jordan, C., Perola, G. C., Roeder, R. C. & Schmidt, M., 1978. *Nature*, **275**, 404.

Cannon, R. D., Penston, M. V. & Brett, Rosemary, A., 1971. *Mon. Not. R. astr. Soc.*, **152**, 79.

Cavaliere, A. & Morrison, P., 1980. *Astrophys. J.*, **238**, L63.

Davidsen, A. F. & Hartig, G. F., 1978. Paper read at *COSPAR/IAU Symp. on X-ray Astronomy, Innsbruck, June 1978.*

Fosbury, R. A. E., Snijders, M. A. J., Boksenberg, A. & Penston, M. V., 1981. *Mon. Not. R. astr. Soc.*, **197**, 235.

Giacconi, R., Branduardi, G., Briel, U., Epstein, A., Fabricant, D., Feigelson, E., Forman, W., Gorenstein, P., Grindlay, J., Gursky, H., Harnden, F. R. Jr., Henry, J. P., Jones, C., Kellogg, E., Koch, D., Murray, S., Schreier, E., Seward, F., Tananbaum, H., Topka, K., Van Speybroeck, L., Holt, S. S., Becker, R. H., Boldt, E. A., Serlemitsos, P. J., Clark, G., Canizares, C., Markert, T., Novick, R., Helfand, D. & Long, K., 1979. *Astrophys. J.*, **230**, 540.

Grindlay, J. E., Marshall, H. L., Hertz, P., Soltan, A., Weisskopf, M. C., Elsner, R. E., Ghosh, P., Darbro, W. & Sutherland, P. G., 1980. *Astrophys. J.*, **240**, L121.

Ives, J. C., Sanford, P. W. & Penston, M. V., 1976. *Astrophys. J.*, **207**, L159.

Lawrence, A., 1980. *Mon. Not. R. astr. Soc.*, **192**, 83.

Lebofsky, M. J. & Rieke, G. H., 1980. *Nature*, **284**, 410.

Maraschi, L., Perola, G. C., Reina, C. & Treves, A., 1979. *Astrophys. J.*, **230**, 243.

Mushotzky, R. F., Holt, S. S. & Serlemitsos, P. J., 1978. *Astrophys. J.*, **255**, L115.

Mushotzky, R. F., Marshall, F. E., Boldt, E. A., Holt, S. S. & Serlemitsos, P. J., 1980. *Astrophys. J.*, **235**, 377.

Penston, M. V., Penston, M. J., Selmes, R. A., Becklin, E. E. & Neugebauer, G., 1974. *Mon. Not. R. astr. Soc.*, **169**, 357.

Penston, M. V., Boksenberg, A., Bromage, G. E., Clavel, J., Elvius, A., Gondhalekar, P. H., Jordan, C., Lind, J., Lindegren, L., Perola, G. C., Pettini, M., Snijders, M. A. J., Tanzi, E. G., Tarenghi, M. & Ulrich, M. H., 1981. *Mon. Not. R. astr. Soc.*, **196**, 857.

Perola, G. C. & Tarenghi, M., 1980. *Astrophys. J.*, **240**, 447.

Rees, M. J., 1979. In *X-Ray Astronomy*, p. 377, eds Giacconi, R. & Setti, G., Reidel, Dordrecht.

Rieke, G. H. & Lebofsky, M. J., 1981. *Astrophys. J.*, **250**, 87.

Seaton, M. J., 1979. *Mon. Not. R. astr. Soc.*, **187**, 73P.

Schmidt, G. D. & Miller, J. S., 1980. *Astrophys. J.*, **240**, 759.

Snijders, M. A. J., 1980. *SERC IUE Newsletter, No. 5*, p. 85.

Sunyaev, R. A. & Titarchuk, L. G., 1980. *Astr. Astrophys.*, **86**, 121.

Thompson, I., Landstreet, J. D., Angel, J. R. P., Stockman, H. S., Woolf, N. J., Martin, P. G., Maza, J. & Beaver, E. A., 1979. *Astrophys. J.*, **229**, 909.

Ulrich, M. H., Boksenberg, A., Bromage, G., Carswell, R., Elvius, A., Gabriel, A., Gondhalekar, P. M., Lind, J., Lindegren, L., Longair, M. S., Penston, M. V., Perryman, M. A. C., Pettini, M., Perola, G. C., Rees, M., Sciama, D., Snijders, M. A. J., Tanzi, E. G., Tarenghi, M. & Wilson, R., 1980. *Mon. Not. R. astr. Soc.*, **192**, 561.

Appendix

In all the spectra taken since 1979 May 3, the flux in the interval $\lambda\lambda$1980–2200 lies systematically above the extrapolation of the power law fitting the six continuum points longward of λ2200. The excess above the fit varies from date to date about a mean value of $3.8 \times 10^{-12}\,\mathrm{erg\,cm^{-2}\,s^{-1}}$, with a standard deviation of 35 per cent, but remains practically constant (within seven per cent) in spectra taken during the same shift. We have considered the following possible explanations but the origin of the excess still is not clear: a) The excess is associated with the short wavelength component. This possibility seems excluded by the lack of correlation both with the excess at λ1455 and the slope defined by the two points at $\lambda\lambda$1710 and 1455. b) Since the LW camera sensitivity is lowest at wavelengths shorter than λ2200, an underestimate of the background in this region of the spectrum could have led us to a conspicuous overestimate of the flux. Then one would expect the same scatter among the excess values measured during the same shift and in different shifts, contrary to what is found. c) The excess is due to a number of variable emission lines, which are difficult to recognize because they fall in the noisiest part of the LW spectra. Then one would expect a correlation with the intensity variations observed in other emission lines, which is not found. d) The effect is caused by variable absorption associated with the dust responsible for infrared variations observed by Lebofsky & Rieke (1980). This appears in contradiction with the fact that the effect is seen only on the short wavelength side of the λ2200 feature.